THE JOURNAL OF PHYSICAL CHEMISTRY Letters

Letter

pubs.acs.org/JPCL

Adsorption and Deposition of Li_2O_2 on TiC{111} Surface

Zhenyu Wang,[†] Jianwei Sun,[‡] Yonghong Cheng,[†] and Chunming Niu*,[†]

[†]Center of Nanomaterials for Renewable Energy, State Key Lab of Electrical Insulation and Power Equipment, School of Electrical Engineering, Xian Jiaotong University, 99 Yanxiang Road, Xian 710054, China

[‡]Department of Physics, Temple University, 1900 North 13th Street, Philadelphia, Pennsylvania 19122, United States

Supporting Information

ABSTRACT: A recent experimental study from Bruce's group demonstrated the feasibility of TiC as a cathode material for Li air battery. We investigate Li_2O_2 adsorption and deposition on TiC{111} surface by periodic density functional theory calculation. The results showed that, upon interaction with Ti-terminated TiC{111} surface, Li_2O_2 clusters reassembled into a saturated periodic two atomic layer coating in which each O atom was bonded to three Ti atoms to form a O layer equivalent to the layer formed by O_2 surface oxidation, and the Li atoms sat on the top. The atomic arrangement of O and Li layers is the same as that of O2Li1 layers normal to ⟨0001⟩ direction in Li_2O_2 crystal structure. Interface models constructed based on this lead showed that the growth of Li_2O_2 can be continued through a surface conduction mechanism to form Li_2O_2 coating with lattice parameters almost identical to those of the standard Li_2O_2 unit cell. The results support the experimental discovery from Bruce's group.

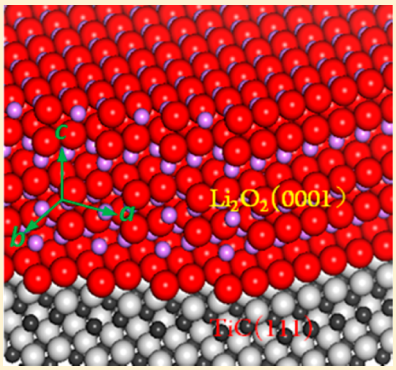

SECTION: Molecular Structure, Quantum Chemistry, and General Theory

Li air (O_2) batteries reported first by Abraham and Jiang[1] are continuously attracting great attention because of their high specific theoretical energy and potential to meet the demand of high energy density for applications such as the power source for next generation of the electric vehicles. The chemistry of Li air batteries is simple, relying largely on reversible deposition and decomposition of Li_2O_2 on the surface of cathode.[2−4] To date, the cathode remains a great barrier[5] to making Li air battery practical. The cathode needs to be conducting for electron transport, highly porous to accommodate the deposition of discharge product Li_2O_2, and stable but with sufficient active surface sites to effectively facilitate the formation and decomposition of Li_2O_2 during charge and discharge cycle. The porous carbon has been widely studied as the cathode materials. Unfortunately, carbon is not stable. It is known that electrochemical oxidization[6] of carbon occurs above 4 V versus Li/Li^+. As a cathode material for the aprotic Li_2O_2 cell, the carbon is more problematic, decomposing at even lower voltage (>3 V) because of highly reactive free radicals involved during O_2 reduction (discharge) and Li_2O_2 oxidation (charge).[7−11] Additionally, carbon also catalyzes the decomposition of aprotic electrolytes.[9−11] Both processes form Li_2CO_3 which deposits on the surface of cathode, resulting in rapid cell performance degradation. Improvement has been reported by using catalysts[2,12−19] such as MnO_2, Au, and Pt in the cathode, but the issues remain. Bruce's group showed that nanoporous gold cathode when combined with an electrolyte based on dimethyl sulfoxide (DMSO) exhibits very good stability.[20] Unfortunately, the high mass density of gold cathode reduces specific energy density, which takes away the key advantage of high specific energy provided by Li air cell over Li ion. Furthermore, gold is too expensive to be commercially viable. Recently, the same group reported[21] that a cathode based on TiC can overcome the disadvantages of carbon and nanoporous gold. It greatly reduces side reactions at the electrolyte−cathode interface compared with carbon, is more stable than nanoporous gold, and delivers >99.5% purity of Li_2O_2 formation on each discharge and its complete oxidation on charge, with >98% capacity retention after 100 cycles. They attributed this excellent performance to electric conductivity of TiC and the formation of an oxide layer on the surface of TiC.

We investigate Li_2O_2 adsorption and deposition on TiC{111} surface by periodic density functional theory calculation. The results showed that surface oxidation plays an important role in Li_2O_2 nucleation and growth initiation on Ti-terminated TiC{111} surface, and continued electrochemical growth of Li_2O_2 along its ⟨0001⟩ direction on TiC{111} surface is feasible because an electron path is provided through surface conduction of Li_2O_2{0001} surface despite the insulation nature of Li_2O_2 bulk.

TiC{111} surface could be terminated[22] with either a layer of C atoms or a layer of Ti atoms. The C-terminated Ti{111} surface is not stable, destroyed by interaction with Li_2O_2 clusters (Figure s1a in the Supporting Information). Figure 1a shows relaxed structure of single and double Li_2O_2 cluster adsorbed on 2 × 2 Ti-terminated TiC{111} surface. The initial adsorption models (Figure s1b in the Supporting Information)

Received: August 22, 2014
Accepted: October 27, 2014

   dx.doi.org/10.1021/jz501775a | J. Phys. Chem. Lett. 2014, 5, 3919−3923

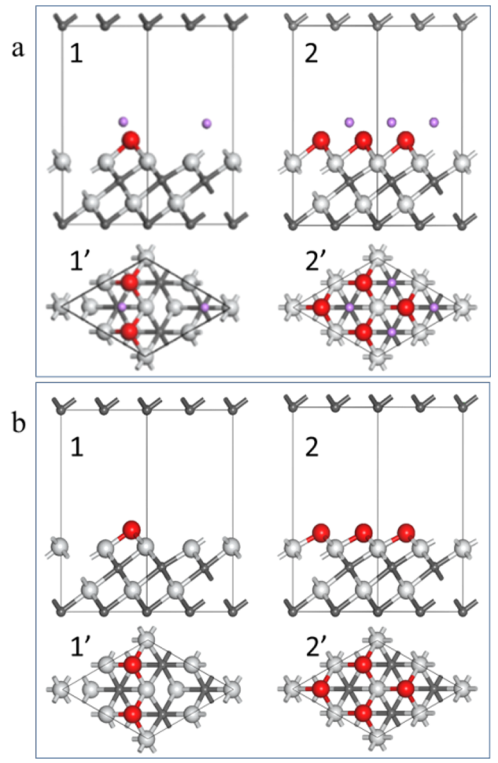

Figure 1. (a) Li_2O_2 adsorption and reaction on 2 × 2 Ti-terminated TiC{111} surface. Side and top views of 1 and 1′, single Li_2O_2 and 2 and 2′, double Li_2O_2. (b) Oxygen adsorption and reaction on 2 × 2 Ti-terminated TiC{111} surface. Side and top views of 1 and 1′, single O_2 and 2 and 2′, double O_2. White sphere, Ti; red sphere, O; grey sphere, C; pink sphere, Li.

were created by placing planar Li_2O_2 clusters on Ti-terminated TiC{111} surface in parallel. The planar Li_2O_2 structure was first reported by Lau et al.,[23] in which two O atoms and two Li atoms sit at opposite corners of a rhombus parallelogram with a O−O bond length of 1.56 Å (Figure s2c in the Supporting Information). Note that O atoms in Li_2O_2 crystals are also paired[24−26] with slightly smaller O−O band length of 1.55 Å. For both single and double Li_2O_2 adsorption, regardless of the initial configurations, a complete breakdown of Li_2O_2 planar structure and rearrangement of O and Li atoms took place. The O atoms moved to the hcp hollows of facial Ti termination, for double Li_2O_2 adsorption, forming an saturated periodic O layer with each O atom bonded to three Ti atoms (Figure 1a, 2,2′), and the Li atoms moved to fcc hollows of extrapolated C atom positions, for double Li_2O_2 adsorption, forming a saturated Li layer on top of the O layer. By comparison of O and Li atom arrangement in O layer and Li layer with that in Li_2O_2 crystal (Figure s3 in the Supporting Information), it can be seen that the O atom layer and Li atom layer are almost identical to O2Li1 layers normal to Li_2O_2 ⟨0001⟩ direction in Li_2O_2 crystal structure. This great structure similarity suggests a nucleation initiation of Li_2O_2 and the beginning of Li_2O_2 epitaxial growth on Ti-terminated TiC{111} surface.

Mulliken bond overlap population analysis results are shown in Table 1. The average Ti−O bond length is 2.234 and 2.252 Å for single Li_2O_2 and double Li_2O_2 adsorption, respectively, which are longer than Ti−O bond length of 1.91 to 2.04 Å in TiO_2 oxide.[27] The calculated bond populations for Ti−O bond are all positive, suggesting attractive interaction. The average overlap population of Ti−Li bonds is all negative. This can be explained by the electrostatic repulsion between positive charged Li and Ti atoms. Consistent with Mulliken population analysis, local density of states (LDOS) calculation showed (Figure s4 in the Supporting Information) that upon Li_2O_2 adsorption the distribution of Ti-3d DOS changed substantially across the spectrum. The four peaks above Fermi level were reduced to three, and DOS at Fermi level was reduced and spread downward to −7 eV. Between 2 and 7 eV, there is overlap between Ti-3d and O-2p states. The DOS of O-2p is largely localized between −4 and −7 eV, and the DOS of Li-1s2s is largely distributed near and above Fermi level. The calculated adsorption energy for single Li_2O_2 cluster adsorption is −10.572 eV per Li_2O_2, slightly decreased to −10.056 eV per Li_2O_2 for double Li_2O_2 cluster adsorption.

To further understand Ti−O bond nature, we also carried out study of O_2 adsorption on Ti-terminated TiC{111} surface. We found that Ti-terminated TiC{111} surface is readily oxidized by interaction with O_2 molecules. The relaxed structures of single O_2 and double O_2 adsorption on 2 × 2 Ti-terminated TiC{111} surface are shown in Figure 1b. In both cases, O_2 molecule decomposes. Similar to the Li_2O_2 adsorption, O atoms moved to the hcp hollows of the facial Ti termination, for double O_2 adsorption, forming a saturated periodic O layer with each O atom bonded to three Ti atoms. The calculated average Ti−O bond length is 1.988 and 1.984 Å for single and double O_2 adsorption, respectively, very much similar to the Ti−O bond length of 1.91 to 2.04 Å in TiO_2 oxide.[27] It has been known that the TiC surface is not stable toward oxidation. Shirotori et al.[28] investigated TiC{100} surface by XPS and LEED and found that when the TiC surface is exposed to O_2 at room temperature the C atoms in the TiC substrate are depleted and the Ti atoms are oxidized to form a disordered TiO_x ($1.5 < x < 2.0$) layer.

We calculated the surface energy of Ti-terminated TiC{111}_Ti surface before and after this oxidation, and we found that the surface energy of Ti-terminated TiC{111} is 208 meV/Å^2, a little higher than the reported value[29] of 194 meV/Å^2, which decreased to 39 meV/Å^2 after oxidation, a significant surface stability improvement. Bruce's group[21] in their report showed that the surface of their as-received TiC contained significant proportions of TiO_2 and TiOC. The proportion of TiO_2 increased further upon the first discharge and remained the same thereafter.

Table 1. Li_2O_2 Cluster Adsorption on TiC Surface: Average Bond Length, Mulliken Overlap Population and Adsorption Energy

surface	n Li_2O_2[a]	bond	L_{max}(A−B)/Å	L_{min}(A−B)/Å	$\bar{L}$/Å	$\bar{n}$	E_{ad}/eV[b]
TiC{111}_Ti	1	Ti−O	2.236	2.229	2.234	0.35	−10.572
		Ti−Li	2.927	2.760	2.849	−0.13	
TiC{111}_Ti	2	Ti−O	2.271	2.242	2.252	0.42	−10.056
		Ti−Li	2.806	2.773	2.794	−0.21	

[a]Number of Li_2O_2 clusters adsorbed on 2 × 2 TiC{111}_Ti surface. [b]Adsorption energy.

dx.doi.org/10.1021/jz501775a | J. Phys. Chem. Lett. 2014, 5, 3919−3923

Because of strong bonding of O atoms to Ti atoms of TiC{111} surface and the significant surface stability improvement after O layer addition to the Ti-terminated Ti{111} surface, next we considered this oxidized Ti-terminated TiC{111} surface, denoted as TiC{111}_Ti_O, as the substrate to build interface models to investigate Li_2O_2 deposition. Both TiC{111} surface and Li_2O_2{0001} surface were hexagonal.[22,24−26] A relatively small misfit factor of 3.65% was calculated between two lattices. To match TiC{111}_Ti_O with Li_2O_2{0001}, we used Li−O bonding as the interface and added a four atomic layer stack of O2Li3O4Li1 (4 Li_2O_2) to the top of the O layer of the 2 × 2 TiC{111}_Ti_O substrate (symmetric nine atomic layer slab with two O layers, four Ti layers, and three C layers, total of 36 atoms) to build the first interface model of 1 ML. Note that O2Li3O4Li1 is equivalent to a monolayer of stoichiometric Li_2O_2 in the Li_2O_2 crystal structure (Figure s3 in the Supporting Information). To get a symbolic sense of continued growth of Li_2O_2, we then added additional O2Li3O4Li1 monolayer sequentially to create 2 and 3 ML models. In this manner of the addition, we avoided breaking O−O bonds of O−O pairs (bond length: 1.55 Å, >1.21 Å of O_2 molecule), which is how O atoms present in the Li_2O_2 structure, and ensured that the surface termination of the Li_2O_2 coating is consistent with $O_2Li_3O_4$ of Li_2O_2{0001}. To avoid polarization effect, the Li_2O_2 coating was applied to both sides of the symmetric nine layer TiC{111}_Ti_O slab for all three models. Note that bulk Li_2O_2 is an insulator. However, Radin et al.[30,31] found that oxygen-rich termination in the Li_2O_2 ⟨0001⟩ direction is the most stable at 300 K and the most stable surface overall of Li_2O_2 crystal structure. Because of the reduced coordination of oxygen atoms at this Li_2O_2 surfaces, a thin metallic and ferromagnetic region (i.e., half-metallic behavior) localized at the surface was formed, with an estimated electrical conductivity of ~10^5 Ω^{-1}/m. This surface conduction was confirmed by our calculation and provides an electron pathway for continuously electrochemical deposition of Li_2O_2 otherwise prohibitive. Figure 2a−c shows relaxed structure for 1 ML, 2 ML, and 3 ML models, respectively. During the relaxation, we allowed all atoms except c atoms in the center of the TiC substrate to move and find their thermal equilibrium positions. The convergence was reached easily for all three models. Figure 3 compares a cut-out unit cell (Figure 3a) form the relaxed 3 ML model (Figure 2c) to the unit cell of pure Li_2O_2 (Figure 3b) determined by our calculation and the unit cell accepted as the standard[26] (Figure 3c). It can be seen that atomic layer distances in this cut-out are very close to those from both the standard, and our calculation of pure Li_2O_2 indicated that after the first layer of O2Li3O4Li1 deposition the structure of Li_2O_2 coating becomes almost the same as that of bulk Li_2O_2. There are two types of Li atoms in the Li_2O_2 coating, Li1 located between O−O pair layer and Li3 located inside the O−O pair layer (Figure S2 in the Supporting Information). Mulliken atom population analysis showed that Li3 was almost 100% ionic, giving up nearly the entire 2s electron, and Li1 was partially covalent with a positive charge from 0.78 to 0.88. We carried out Mulliken band overlap population analysis for Li−O interface bonding between TiC{111}_Ti_O surface and Li_2O_2 coating. The overlap population for Li−O band was 0.46, and average bond length was 2.063, 2.100, and 2.101 Å for 1, 2, and 3 ML models, respectively. The ideal work of adhesion W_{ad} of Li_2O_2 coating to Ti{111}_Ti_O surface calculated was 224, 224, and 222 meV/Å^2 for 1, 2, and 3 ML, respectively. We also calculated LDOS distribution for all three models across the Fermi level. A common feature of LDOS of three models is that the surface of Li_2O_2 coating is always conducting and the density state at the Fermi level is mainly from O-2p states. Figure 4 shows layer-projected LDOS distribution of the 3 ML model from TiC substrate interior, across the interface, and through the Li_2O_2 coating to the top of the surface. It can be seen that the TiC{111}_Ti surface remains conductive after O layer addition. The Ti-3d states are largely responsible for the conductivity of TiC{111}_Ti_O substrate surface. After the

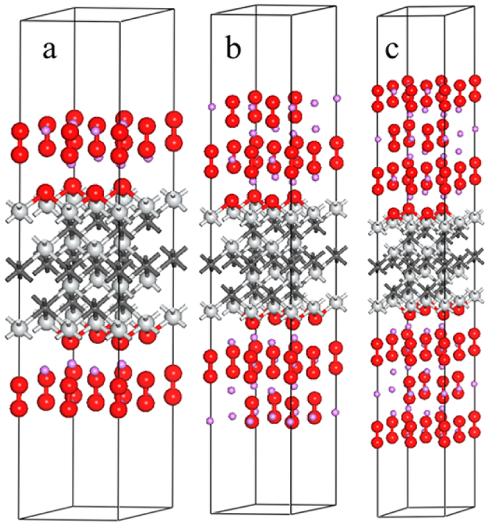

Figure 2. Relaxed interface models of Li_2O_2{0001}_$O_2Li_3O_4$ with TiC{111}_Ti_O surface: (a) 1 ML, (b) 2 ML, and (c) 3ML. White sphere, Ti; red sphere, O; grey sphere, C; pink sphere, Li.

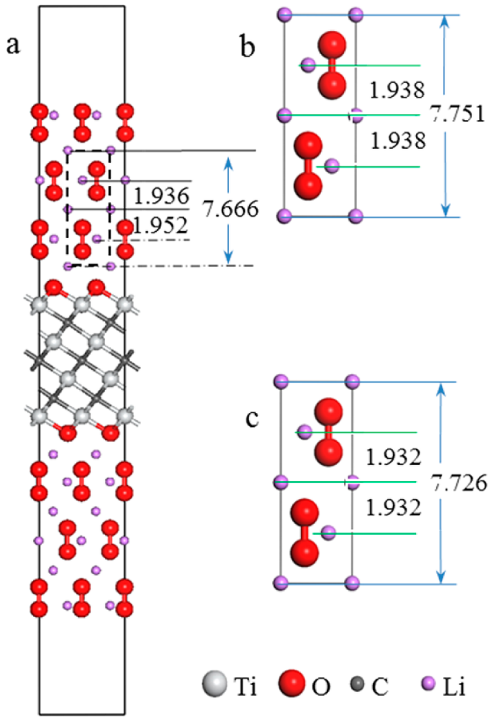

Figure 3. Comparison of (a) unit cell parameters of calculated from Li_2O_2 coating on Ti{111}_Ti_O calculated from (b) bulk Li_2O_2 and from (c) standard unit cell of Li_2O_2.

dx.doi.org/10.1021/jz501775a | J. Phys. Chem. Lett. 2014, 5, 3919−3923

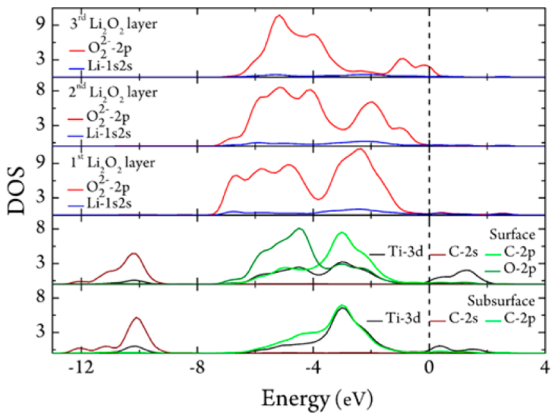

Figure 4. Layer-projected LDOS of Li_2O_2 coating on TiC{111}_Ti_O surface, 3 ML model.

first layer of Li_2O_2 deposition, the DOS at Fermi level decreased. After the second layer, consistent with the lattice structure evolution (Figure 3a), the electronic structure of Li_2O_2 coating also became bulk Li_2O_2-like, the DOS at Fermi level diminished, the interior coating became insulating, while the surface of the coating after the third layer deposition remained conducting. The surface conductivity provided an electron path for electrochemical growth of Li_2O_2.

There is still a debate how large Li_2O_2 crystallites are formed electrochemically considering that Li_2O_2 bulk is an insulator. The theoretical model suggested that conduction relying on electron tunneling can only support 5−10 nm thick Li_2O_2 formation.[32] Our above result clearly shows that on TiC{111}_Ti_O surface, continuous growth Li_2O_2 coating along its ⟨0001⟩ direction is feasible via a surface electron mechanism. The surface electron conduction mechanism was proposed first by Radin et al.[30] based on DFT calculation using PBE functional, further confirmed by their calculation using HSE06 hybrid functional and quasiparticle GW methods.[31] Others showed that lithium vacancies in the bulk[33,34] and some grain boundaries[35] could also induce conductivity in Li_2O_2. Note that to describe vacancy states more accurately, Varley et al. used HSE hybrid functional.[33] At this point, all of these results suggest that it is possible to grow thick Li_2O_2 electrochemically, a prerequisite for a practical Li air battery. However, the critical question of whether these conduction paths are sufficient to sustain a high current when a thick Li_2O_2 is involved is still uncertain,[36,37] requiring further theoretical and experimental studies.

In summary, our computational results showed that upon interaction with Ti-terminated TiC{111} surface planar Li_2O_2 cluster decomposes and Li and O atoms rearrange, in the case of double Li_2O_2 adsorption on a 2 × 2 TiC{111} surface lattice, to form a saturated periodic two-layered structure with a O layer bonded to Ti atoms of the TiC{111} surface and a Li layer bonded on top of the O layer. Atomic positions of both Li and O atoms in this surface structure are almost identical to that in O2Li1 layers in the Li_2O_2 crystal normal to its ⟨0001⟩ direction. Hence, the results suggest Li_2O_2 nucleation and the beginning of epitaxial growth of Li_2O_2 coating. For comparison, we also investigated O_2 interaction and oxidation reaction with Ti-terminated TiC{111} surface; a similar saturated O layer was formed by double O_2 adsorption on Ti-terminated 2 × 2 TiC{111} surface lattice. The surface oxidation lead to significant surface energy reduction from 208 to 39 meV/Å^2, a great improvement of the stability of Ti-terminated TiC{111} surface. Following the lead from the studies of Li_2O_2 and O_2 adsorption, we used oxidized Ti-terminated TiC{111} surface instead of the pristine one to construct interface models by adding a four atomic layer stack of O2Li3O4Li1 (equivalent to a stoichiometric layer of Li_2O_2 normal to ⟨0001⟩ direction in the Li_2O_2 crystal) sequentially. The result showed that continued electrochemical growth of Li_2O_2 on oxidized Ti-terminated TiC{111} is feasible through a surface conduction mechanism.

This study represents first theoretical treatment of Li_2O_2 nucleation and growth on TiC electrode. It is clear that surface oxidation of TiC{111}, which significantly improves the stability of TiC, and conductivities of oxidized TiC and O-terminated Li_2O_2{0001} surface all play an important role in Li_2O_2 coating growth. The results support the experimental discovery from Bruce's group.

■ ASSOCIATED CONTENT

Supporting Information

Calculation details. Side and top views of double Li_2O_2 adsorption on C-terminated TiC{111} surface before and after relaxation and single Li_2O_2 and double Li_2O_2 adsorption on Ti-terminated TiC{111} models before relaxation. Cubic crystallographic structure of TiC, hexagonal crystallographic structure of Li_2O_2, and planar structure of Li_2O_2 cluster. Labeling scheme for unique atom layer in the Li_2O_2 structure. Angular momentum projected LDOS distribution for atoms at interface and subinterface. This material is available free of charge via the Internet at http://pubs.acs.org.

■ AUTHOR INFORMATION

Corresponding Author

*E-mail: cniu@mail.xjtu.edu.cn.

Notes

The authors declare no competing financial interest.

■ ACKNOWLEDGMENTS

Financial support was provided by Xian Jiaotong University through a grant for the establishment of the Center of Nanomaterials for Renewable Energy and a CNSF grant 51221005. We thank Bing Xiao in Department of Physical Chemistry, Temple University for reading the manuscript and providing valuable feedback.

■ REFERENCES

(1) Abraham, K. M.; Jiang, Z. A Polymer Electrolyte-Based Rechargeable Lithium/Oxygen Battery. *J. Electrochem. Soc.* **1996**, *143*, 1−5.

(2) Ogasawara, T.; Debart, A.; Holzapfel, M.; Novak, P.; Bruce, P. G. Rechargeable Li_2O_2 Electrode for Lithium Batteries. *J. Am. Chem. Soc.* **2006**, *128*, 1390−1393.

(3) Zhong, L.; Mitchell, R. R.; Liu, Y.; Gallant, B. M.; Thompson, C. V.; Huang, J. Y.; Mao, S. X.; Shao-Horn, Y. In Situ Transmission Electron Microscopy Observations of Electrochemical Oxidation of Li_2O_2. *Nano Lett.* **2013**, *13*, 2209−2214.

(4) Read, J.; Mutolo, K.; Ervin, M.; Behl, W.; Wolfenstine, J.; Driedger, A.; Foster, D. Oxygen Transport Properties of Organic Electrolytes and Performance of Lithium/oxygen Battery. *J. Electrochem. Soc.* **2003**, *150*, A1351−A1356.

(5) Li, F. J.; Zhang, T.; Zhou, H. S. Challenges of Non-Aqueous Li-O_2 Batteries: Electrolytes, Catalysts, and Anodes. *Energy Environ. Sci.* **2013**, *6*, 1125−1141.

(6) Kim, J.; Lee, J.; Tak, Y. Relationship between Carbon Corrosion and Positive Electrode Potential in a Proton-exchange Membrane Fuel Cell during Start/Stop Operation. *J. Power Sources* **2009**, *192*, 674−678.
(7) Freunberger, S. A.; Chen, Y. H.; Peng, Z. Q.; Griffin, J. M.; Hardwick, L. J.; Barde, F.; Novak, P.; Bruce, P. G. Reactions in the Rechargeable Lithium-O_2 Battery with Alkyl Carbonate Electrolytes. *J. Am. Chem. Soc.* **2011**, *133*, 8040−8047.
(8) McCloskey, B. D.; Bethune, D. S.; Shelby, R. M.; Girishkumar, G.; Luntz, A. C. Solvents' Critical Role in Nonaqueous Lithium-oxygen Battery Electrochemistry. *J. Phys. Chem. Lett.* **2011**, *2*, 1161−1166.
(9) McCloskey, B. D.; Speidel, A.; Scheffler, R.; Miller, D. C.; Viswanathan, V.; Hummelshøj, J. S.; Norskov, J. K.; Luntz, A. C. Twin Problems of Interfacial Carbonate Formation in Nonaqueous Li-O_2 Batteries. *J. Phys. Chem. Lett.* **2012**, *3*, 997−1001.
(10) Bruce, P. G.; Freunberger, S. A.; Hardwick, L. J.; Tarascon, J.-M. Li-O_2 and Li-S Batteries with High Energy Storage. *Nat. Mater.* **2012**, *11*, 19−29.
(11) Ottakam Thotiyl, M. M.; Freunberger, S. A.; Peng, Z.; Bruce, P. G. The Carbon Electrode in Nonaqueous Li-O_2 Cells. *J. Am. Chem. Soc.* **2012**, *135*, 494−500.
(12) Debart, A.; Bao, J.; Armstrong, G.; Bruce, P. G. An O_2 Cathode for Rechargeable Lithium Batteries: The Effect of a Catalyst. *J. Power Sources* **2007**, *174*, 1177−1182.
(13) Debart, A.; Paterson, A. J.; Bao, J.; Bruce, P. G. Alpha-MnO_2 Nanowires: A Catalyst for the O_2 Electrode in Rechargeable Lithium Batteries. *Angew. Chem., Int. Ed.* **2008**, *47*, 4521−4524.
(14) Thapa, A. K.; Saimen, K.; Ishihara, T. Pd/MnO_2 Air Electrode Catalyst for Rechargeable Lithium/Air Battery. *Electrochem Solid State Lett.* **2010**, *13*, A165−A167.
(15) Thapa, A. K.; Ishihara, T. Mesoporous α-MnO_2/Pd Catalyst Air Electrode for Rechargeable Lithium-Air Battery. *J. Power Sources* **2011**, *196*, 7016−7020.
(16) Thapa, A. K.; Shin, T. H.; Ida, S.; Sumanasekera, G. U.; Sunkara, M. K.; Ishihara, T. Gold-Palladium Nanoparticles Supported by Mesoporous beta-MnO_2 Air Electrode for Rechargeable Li-air Battery. *J. Power Sources* **2012**, *220*, 211−216.
(17) Lu, Y. C.; Gallant, B. M.; Kwabi, D. G.; Harding, J. R.; Mitchell, R. R.; Whittingham, M. S.; Shao-Horn, Y. Lithium-Oxygen Batteries: Bridging Mechanistic Understanding and Battery Performance. *Energy Environ. Sci.* **2013**, *6*, 750−768.
(18) Renner, F. U.; Kageyama, H.; Siroma, Z.; Shikano, M.; Schoder, S.; Grunder, Y.; Sakata, O. Gold Model Anodes for Li-ion Batteries: Single Crystalline Systems Studied by In Situ X-ray Diffraction. *Electrochim. Acta* **2008**, *53*, 6064−6069.
(19) Chen, J. Z.; Hummelshøj, J. S.; Thygesen, K. S.; Myrdal, J. S. G.; Norskov, J. K.; Vegge, T. The Role of Transition Metal Interfaces on the Electronic Transport in Lithium-air Batteries. *Catal. Today* **2011**, *165*, 2−9.
(20) Peng, Z. Q.; Freunberger, S. A.; Chen, Y. H.; Bruce, P. G. A Reversible and Higher-Rate Li-O_2 Battery. *Science* **2012**, *337*, 563−566.
(21) Ottakam Thotiyl, M. M.; Freunberger, S. A.; Peng, Z. Q.; Chen, Y. H.; Liu, Z.; Bruce, P. G. A Stable Cathode for the Aprotic Li-O_2 Battery. *Nat. Mater.* **2013**, *12*, 1050−1056.
(22) Villars, P.; Calvert, L. D. *Pearson's Handbook of Crystallographic Data for Intermetallic Phases*; ASM International: Materials Park, OH, 1991.
(23) Lau, K. C.; Assary, R. S.; Redfern, P.; Greeley, J.; Curtiss, L. A. Electronic Structure of Lithium Peroxide Clusters and Relevance to Lithium-Air Batteries. *J. Phys. Chem. C* **2012**, *116*, 23890−23896.
(24) Chan, M. K. Y.; Shirley, E. L.; Karan, N. K.; Balasubramanian, M.; Ren, Y.; Greeley, J. P.; Fister, T. T. Structure of Lithium Peroxide. *J. Phys. Chem. Lett.* **2011**, *2*, 2483−2486.
(25) Föppl, H. Die Kristallstrukturen Der Alkaliperoxyde. *Z. Anorg. Allg. Chem.* **1957**, *291*, 12−50.
(26) Cota, L. G.; de la Mora, P. On the Structure of Lithium Peroxide, Li_2O_2. *Acta Crystallogr., Sect. B: Struct. Sci.* **2005**, *61*, 133−136.
(27) Park, J. Y.; Lee, C.; Jung, K. W.; Jung, D. Structure Related Photocatalytic Properties of TiO_2. *Bull. Korean Chem. Soc.* **2009**, *30*, 402−404.
(28) Shirotori, Y.; Sawada, K.; Ozawa, K.; Edamoto, K.; Otani, S. Photoelectron Spectroscopy Study of the Oxidation of TiC(100). *Jpn. J. Appl. Phys., Part 1* **2003**, *42*, 1725−1731.
(29) Arya, A.; Carter, E. A. Structure, Bonding, and Adhesion at the TiC(100)/Fe(110) Interface from First Principles. *J. Chem. Phys.* **2003**, *118*, 8982−8996.
(30) Radin, M. D.; Rodriguez, J. F.; Tian, F.; Siegel, D. J. Lithium Peroxide Surfaces Are Metallic, While Lithium Oxide Surfaces Are Not. *J. Am. Chem. Soc.* **2012**, *134*, 1093−1103.
(31) Radin, M. D.; Tian, F.; Siegel, D. J. Electronic Structure of Li_2O_2 {0001} Surfaces. *J. Mater. Sci.* **2012**, *47*, 7564−7570.
(32) Viswanathan, V.; Thygesen, K. S.; Hummelshøj, J. S.; Norskov, J. K.; Girishkumar, G.; McCloskey, B. D.; Luntz, A. C. Electrical Conductivity in Li_2O_2 and Its Role in Determining Capacity Limitations in Non-Aqueous Li-O_2 Batteries. *J. Chem. Phys.* **2011**, *135*, 214704.
(33) Varley, J. B.; Viswanathan, V.; Nørskovbcand, J. K.; Luntz, A. C. Lithium and Oxygen Vacancies and Their Role in Li_2O_2 Charge Transport in Li-O_2 Batteries. *Energy Environ. Sci.* **2014**, *7*, 720−727.
(34) Hummelshøj, J. S.; Blomqvist, J.; Datta, S.; Vegge, T.; Rossmeisl, J.; Thygesen, K. S.; Luntz, A. C.; Jacobsen, K. W.; Norskov, J. K. Communications: Elementary Oxygen Electrode Reactions in the Aprotic Li-Air Battery. *J. Chem. Phys.* **2010**, *132*, 071101.
(35) Geng, W. T.; He, B. L.; Ohno, T. Grain Boundary Induced Conductivity in Li_2O_2. *J. Phys. Chem. C* **2013**, *117*, 25222−25228.
(36) Luntz, A. C.; Viswanathan, V.; Voss, J.; Varley, J.; Nørskov, J. K.; Scheffler, R.; Speidel, A. Tunneling and Polaron Charge Transport Through Li_2O_2 in Li-O_2 Batteries. *J. Phys. Chem. Lett.* **2013**, *4*, 3494−3499.
(37) Radin, M. D.; Siegel, D. J. Charge Transport in Lithium Peroxide: Relevance for Rechargeable Metal Air Batteries. *Energy Environ. Sci.* **2013**, *6*, 2370−2379.